GCC185 plays independent roles in Golgi structure maintenance and AP-1–mediated vesicle tethering

Frank C. Brown, Carmel H. Schindelhaim, and Suzanne R. Pfeffer

Department of Biochemistry, Stanford University School of Medicine, Stanford, CA 94305

GCC185 is a long coiled-coil protein localized to the trans-Golgi network (TGN) that functions in maintaining Golgi structure and tethering mannose 6-phosphate receptor (MPR)–containing transport vesicles en route to the Golgi. We report the identification of two distinct domains of GCC185 needed either for Golgi structure maintenance or transport vesicle tethering, demonstrating the independence of these two functions. The domain needed for vesicle tethering binds to the clathrin adaptor AP-1, and cells depleted of GCC185 accumulate MPRs in transport vesicles that are AP-1 decorated. This study supports a previously proposed role of AP-1 in retrograde transport of MPRs from late endosomes to the Golgi and indicates that docking may involve the interaction of vesicle-associated AP-1 protein with the TGN-associated tethering protein GCC185.

Introduction

Mannose 6-phosphate receptors (MPRs) deliver newly synthesized acid hydrolases to the lysosome (Ghosh et al., 2003). These receptors bind cargo at the TGN and are transported to late endosomes via early endosomes, where they release their cargo as a result of the lower pH of this compartment. Subsequently, MPRs are transported back to the TGN to participate in additional rounds of acid hydrolase delivery (Braulke and Bonifacino, 2009). Transport of MPRs from late endosomes to the TGN has been shown to require several proteins, including Rab9 (Lombardi et al., 1993; Riederer et al., 1994), TIP47 (Díaz and Pfeffer, 1998; Aivazian et al., 2006), a SNARE complex that includes Syntaxin 10, Syntaxin 16, Vti1a, and VAMP3 (Ganley et al., 2008), RhoBTB3 ATPase (Espinosa et al., 2009), and GCC185 (Reddy et al., 2006; Derby et al., 2007).

GCC185 is a Golgi-localized protein that is predicted to form a long coiled-coil structure that protrudes from the Golgi surface (Luke et al., 2003). GCC185 is needed for Golgi structure maintenance; if depleted from cells, the Golgi is transformed from a normal ribbon structure into a cluster of smaller ministacks (Reddy et al., 2006; Derby et al., 2007). This phenotype is common to the loss of any one of several Golgin proteins (Pfeffer, 2010). Additionally, GCC185 functions as a tether for MPR-containing vesicles inbound from late endosomes to the TGN; cells depleted of GCC185 accumulate MPR cargo in Rab9-decorated peripheral transport vesicle carriers (Reddy et al., 2006).

For GCC185 to tether MPR-containing transport vesicles, it must simultaneously bind to proteins on the TGN surface and proteins on the vesicles. The cooperative binding of Rab6 and Arl1 GTPases to the C terminus of GCC185 localizes and anchors the tether to the TGN (Burguete et al., 2008). Later work identified multiple Rab GTPase binding sites across the length of GCC185 that may facilitate MPR vesicle tethering (Sinka et al., 2008; Hayes et al., 2009).

In this study, we report identification of distinct GCC185 domains that are required for either maintenance of Golgi structure or tethering of MPR transport vesicles, demonstrating that the two functions of the protein are independent of one another. In addition, we show that a GCC185 domain required for vesicle tethering comprises a binding site for the clathrin adaptor protein AP-1. Clathrin adaptor proteins participate in packaging transport vesicles by binding the cytoplasmic domains of specific cargo proteins and concomitantly recruiting a clathrin coat (Edeling et al., 2006). AP-1 binds to the cytoplasmic domains of MPRs (Glickman et al., 1989) but has been thought to function in the export of MPRs from the TGN toward endosomes in conjunction with GGA (Golgi-localized γ-adaptin ear-containing ADP ribosylation factor binding) proteins (Braulke and Bonifacino, 2009). Our findings support the conclusion that AP-1 functions additionally in the transport of MPRs from late endosomes to the TGN, as originally suggested in mouse gene knockout experiments (Meyer et al., 2000).

Correspondence to Suzanne R. Pfeffer: pfeffer@stanford.edu

Abbreviations used in this paper: CLASP, cytoplasmic linker–associated protein; MPR, mannose 6-phosphate receptor; NHS, *N*-hydroxysuccinimide.

The Rockefeller University Press $30.00
J. Cell Biol. Vol. 194 No. 5 779–787
www.jcb.org/cgi/doi/10.1083/jcb.201104019

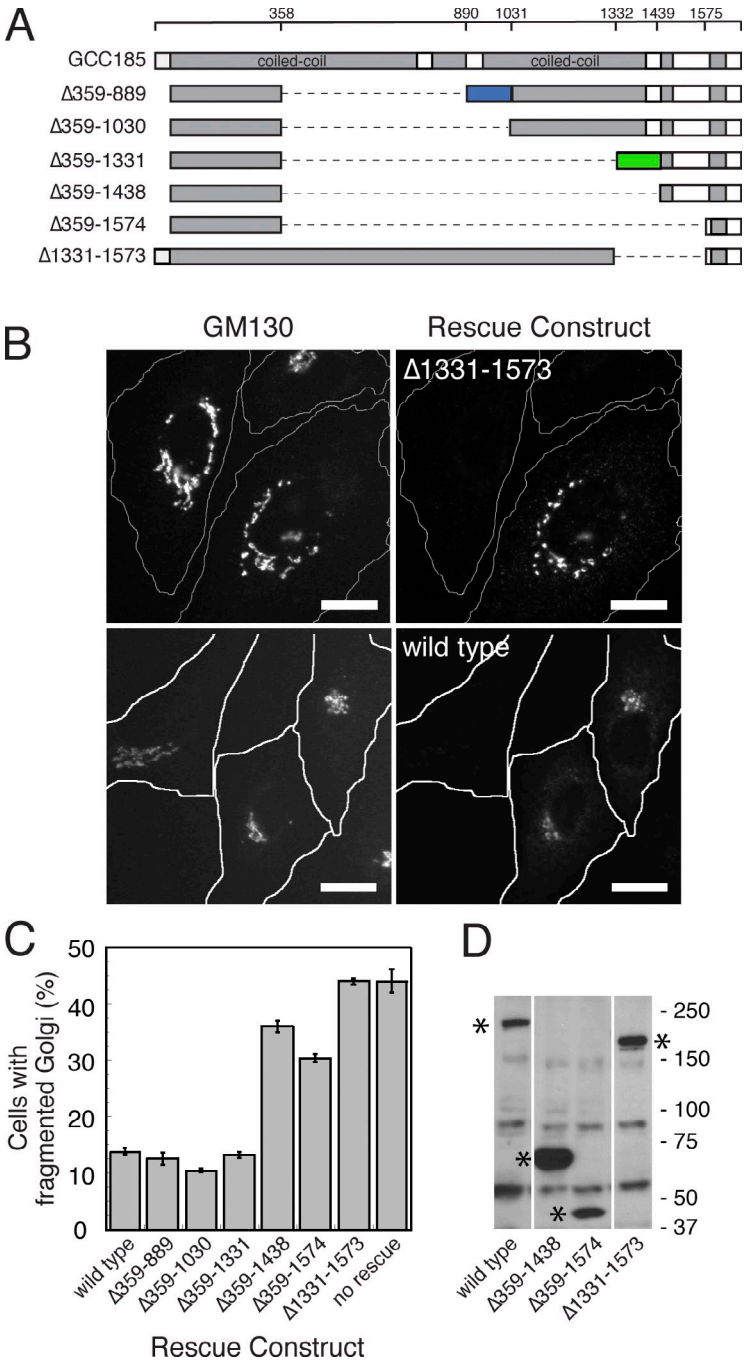

Figure 1. **Maintenance of Golgi ribbon structure requires GCC185 residues 1,332–1,438.** (A) A schematic diagram of GCC185 highlighting the residues predicted to form coiled coils (shown in gray). Truncation constructs used in the depletion and rescue experiments are shown. In blue is a region needed for MPR vesicle tethering; in green is a region needed for maintenance of proper Golgi ribbon structure. Dashed lines represent deleted sequences. (B) Cells were treated with GCC185 siRNA for 72 h. After 48 h of siRNA treatment, cells were transfected with plasmids encoding the indicated siRNA-resistant myc-tagged rescue proteins. (left) Golgi structure assessed using mouse anti-GM130 and Alexa Fluor 488 goat anti–mouse antibodies. (right) GCC185 rescue construct expression detected using chicken anti-myc and Cy3 goat anti–chicken antibodies. Approximate cell outlines are indicated. Bars, 10 µm. (C) Quantification of rescue. The formation of a Golgi ribbon was scored visually by other laboratory members from blinded datasets; the data represent the mean of two experiments in which a total of >45 cells were counted for each construct. Error bars represent SEM from independent experiments. The scoring error between laboratory members was less than a few percent. (D) An immunoblot of the indicated GCC185 constructs (asterisks) after 48 h of expression in HeLa cells. Proteins were detected with anti-myc tag antibody. Three background bands are seen in all lanes. Molecular mass marker mobility is shown at the right in kilodaltons.

Results

Depletion of GCC185 results in the fragmentation of the Golgi into ministacks and the dispersal of MPRs into peripheral transport intermediates (Reddy et al., 2006). A series of truncation constructs was used to explore the contributions of various GCC185 domains toward maintaining Golgi ribbon structure and tethering MPR-containing transport vesicles. Previous work demonstrated a requirement for the first N-terminal coiled-coil domain (residues 1–358) and the absolute C terminus (1,575–1,684) for both of these processes (Hayes et al., 2009). As a starting point for the analysis, we tested a protein lacking ∼30% of the N-terminal coiled-coil regions, a region absent in the *Drosophila melanogaster* GCC185 homologue (Δ359–889). Additional truncations were generated by deleting the protein sequence up to each break in the heptad repeat pattern of the predicted coiled-coil structure (Fig. 1 A).

With regard to GCC185's role in Golgi ribbon structure maintenance, large regions of the molecule could be deleted with little consequence. Thus, constructs missing residues 359–889, 359–1,030, or 359–1,331 were fully competent to rescue altered Golgi morphology (Fig. 1, B and C). Further deletion (359–1,438) generated a molecule that could no longer rescue normal Golgi structure (Fig. 1 C). Consistent with this observation, a GCC185 construct missing just residues 1,331–1,573 also failed to rescue Golgi ribbon morphology (Fig. 1, B and C),

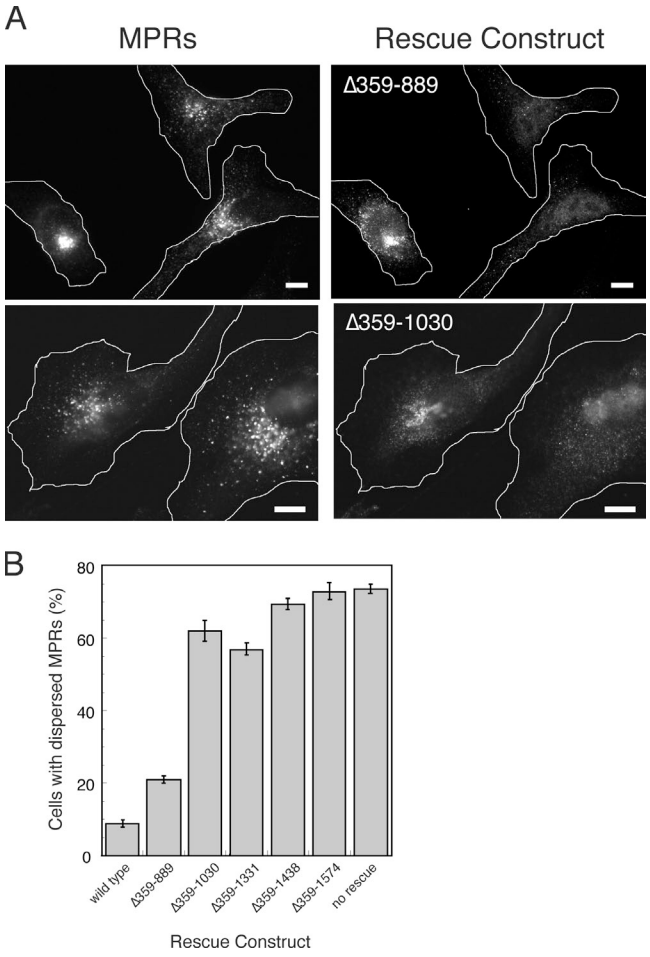

Figure 2. **GCC185 residues 890–1,030 are needed for MPR vesicle tethering.** (A) Cells were treated with GCC185 siRNA for 72 h. After 24 h of siRNA treatment, cells were transfected with plasmids encoding the indicated myc-tagged proteins. (left) MPR localization determined using 2G11 mouse anti-MPR and Alexa Fluor 488 goat anti–mouse antibodies. (right) GCC185 rescue construct expression detected using chicken anti-myc and Cy3 goat anti–chicken antibodies. Approximate cell outlines are indicated. Bars, 10 µm. (B) Quantification of rescue experiments. MPR dispersal was scored visually using blinded datasets; the data represent the mean of at least two experiments in which a total of >45 cells were counted for each condition. Error bars represent SEM from independent experiments.

and, not surprisingly, deletion of residues 359–1,574 also yielded a nonfunctional protein (Fig. 1 C). Failure to rescue Golgi ribbon morphology was not a result of protein expression level differences, which was determined by fluorescence intensity or immunoblotting of transfected cells (Fig. 1 D). These experiments define residues 1,332–1,438 (Fig. 1 A, green box) as a domain needed for GCC185's role in maintenance of the Golgi ribbon.

A central domain needed for transport vesicle tethering

Rescue experiments designed to identify domains needed for MPR vesicle tethering revealed that tethering requires regions other than those needed to maintain Golgi structure. Deletion of residues 359–889 yielded a protein that was capable of restoring normal MPR localization in a majority of cells (Fig. 2, A and B). This construct is similar in size to the *Drosophila* homologue. Further deletion (Δ359–1,030) removed sequences that are needed for MPR transport vesicle consumption at the Golgi but not for Golgi structure maintenance (Fig. 2, A and B). Consistent with this finding, constructs missing residues 359–1,331, 359–1,438, or 359–1,574 were also nonfunctional for vesicle tethering (Fig. 2 B). These experiments identify a region from residues 890–1,030 (Fig. 1 A, blue box) that is essential for GCC185-mediated vesicle tethering.

To further refine the precise determinants needed for vesicle tethering, additional constructs were generated (Fig. 3 A). As expected, deletion of just residues 889–1,032 within the context of the full-length protein yielded a construct that could not rescue vesicle tethering, even though the construct properly localized to the Golgi complex (Fig. 3 C). Residues 890–1,032 are predicted to form an unstructured region (Fig. 3 A, yellow box) followed by a potential coiled coil (Fig. 3 A, blue box). If we deleted just the unstructured region (Fig. 3 A, yellow box) to generate Δ889–939, the protein was functional for vesicle tethering (Fig. 3, B and C); in contrast, deletion of just the adjacent coiled-coil sequences (938–1,032; Fig. 3 A, blue box) yielded a protein that could not rescue the loss of GCC185-mediated vesicle tethering at the TGN (Fig. 3, B and C). Control immunoblots verified that protein expression differences could not account for the failure of transfected proteins to rescue vesicle tethering (Fig. 3 D). These experiments define GCC185 residues 938–1,032 as functioning specifically in transport vesicle tethering.

In previous work, we showed that a fragment comprised of GCC185 residues 805–889 (Fig. 4 A, orange box) could inhibit in vitro transport reactions that reconstitute transport of MPRs from late endosomes to the Golgi (Hayes et al., 2009). In that study, we also identified a Rab9 GTPase binding site within this domain that includes I880 and L873. Because a construct lacking these residues was capable of rescue (Δ359–889; Fig. 2), it seemed unlikely that this Rab9 binding site would be essential for GCC185 function. As expected, GCC185 I880A/L873A was fully functional in restoring vesicle tethering in GCC185-depleted cells (Fig. 4 B). A construct lacking 21 residues of the coiled coil (Δ862–882) was also a wild type in its rescue capacity (Fig. 4, B and C). Thus, although residues 805–889 of GCC185 are not essential for function, a soluble construct representing this domain can interfere with normal GCC185 function (Hayes et al., 2009). Inhibition is likely to have been a result of titration of Rab9 GTPase from in vitro reactions.

Protein interactions needed for GCC185 function

A C-terminal region of GCC185 (residues 1,331–1,438) is needed to maintain Golgi ribbon structure (Fig. 1). Cytoplasmic linker–associated proteins (CLASPs) bind to GCC185 (Efimov et al., 2007) and contribute to maintenance of the Golgi structure (Miller et al., 2009). Therefore, we tested the obvious possibility that GCC185 residues 1,331–1,438 might comprise a CLASP binding site. As shown in Fig. 5 A, GCC185 bound strongly to CLASP1-α or 2-γ, whether or not the protein contained residues 1,331–1,573. This result indicates that the CLASP binding site is located elsewhere on GCC185 and that residues 1,331–1,438 contribute to Golgi structure by a mechanism distinct from CLASP recruitment.

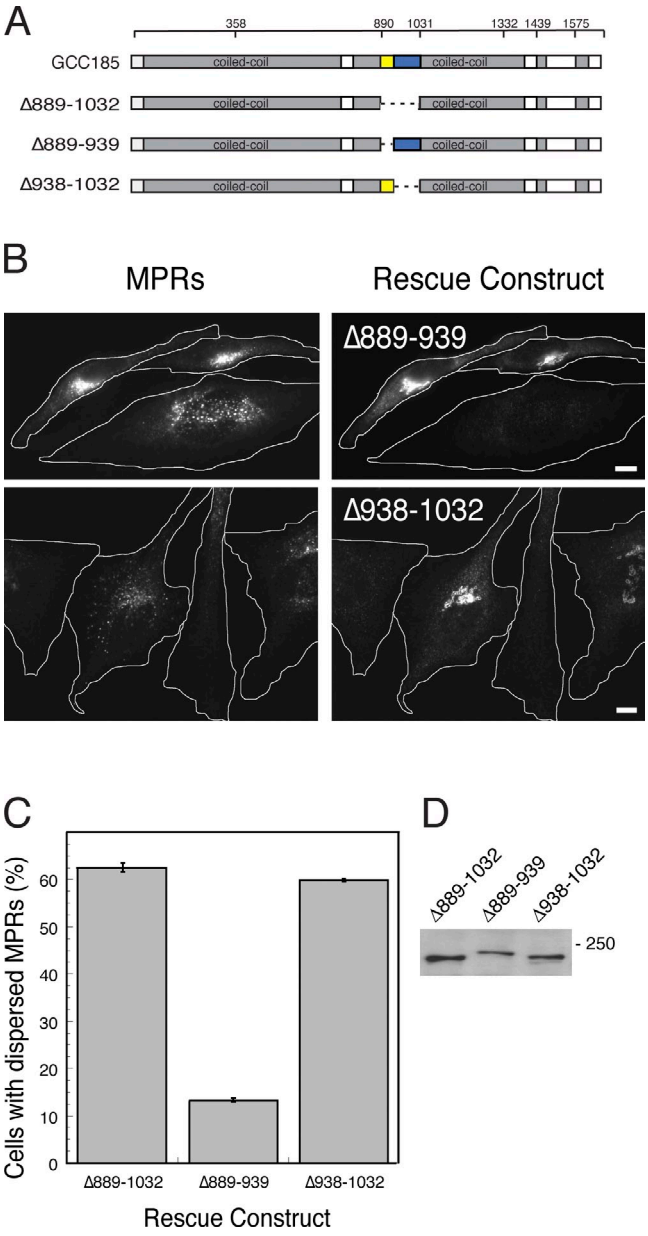

Figure 3. **Coiled-coil residues 939–1,031 are required for MPR vesicle tethering.** (A) A schematic diagram of GCC185 and the truncation constructs used in the depletion and rescue experiments. In blue is a coiled-coil region needed for MPR vesicle consumption; in yellow is an adjacent putative unstructured region. (B) GCC185 depletion and rescue with the indicated constructs as described in Fig. 2. Approximate cell outlines are indicated. Bars, 10 µm. (C) Quantification of rescue. MPR dispersal was scored visually using blinded datasets; the data represent the mean of at least two experiments in which a total of >100 cells were counted for each condition. Error bars represent SEM from independent experiments. (D) An immunoblot of the indicated GCC185 constructs after 48 h of expression in HeLa cells. Proteins were detected with anti-myc tag antibody. Molecular mass marker mobility is shown in kilodaltons.

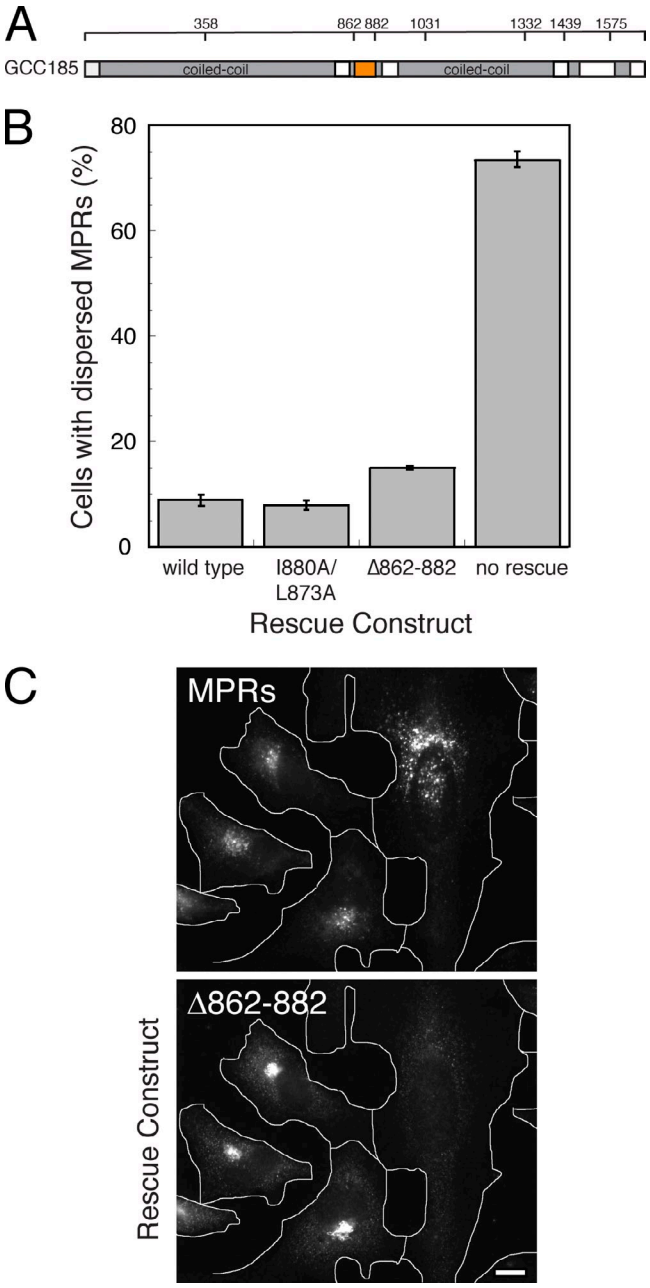

Figure 4. **A Rab9 binding site in coiled-coil 3 is dispensable for vesicle tethering.** (A) A schematic diagram of GCC185. Depicted in orange is a coiled-coil region containing a Rab9 binding site (Hayes et al., 2009). (B) GCC185-depleted cells were rescued and analyzed as described in Fig. 2. The quantification of rescue is shown. MPR dispersal was scored visually from blinded datasets; the data represent the mean of at least two experiments in which a total of >45 cells were counted for each condition. Error bars represent SEM from independent experiments. (C) Representative images. MPR localization (top) and GCC185 rescue with Δ862–882 (bottom) are shown. Approximate cell outlines are indicated. Bar, 10 µm.

GCC185's C terminus is needed for its Golgi localization, a process that is mediated by Rab6 and Arl1 GTPases (Burguete et al., 2008). As for vesicle tethering, GCC185 residues 939–1,031 may bind directly to a constituent of transport vesicles or to another intermediate protein that interacts with vesicles. Therefore, we sought possible binding partners of this domain. The AP-1 clathrin adaptor has been implicated in MPR retrograde transport, as mouse cells lacking this complex accumulate MPRs in early endosomes (Meyer et al., 2000). Therefore, we tested whether purified AP-1 complex binds directly to the region of GCC185 that is needed for MPR transport vesicle tethering.

GST fusion constructs were generated that represent the domain of GCC185 that participates in vesicle tethering (890–1,031, 939–1,031, or 1,032–1,331 as a control; Fig. 5, B and C).

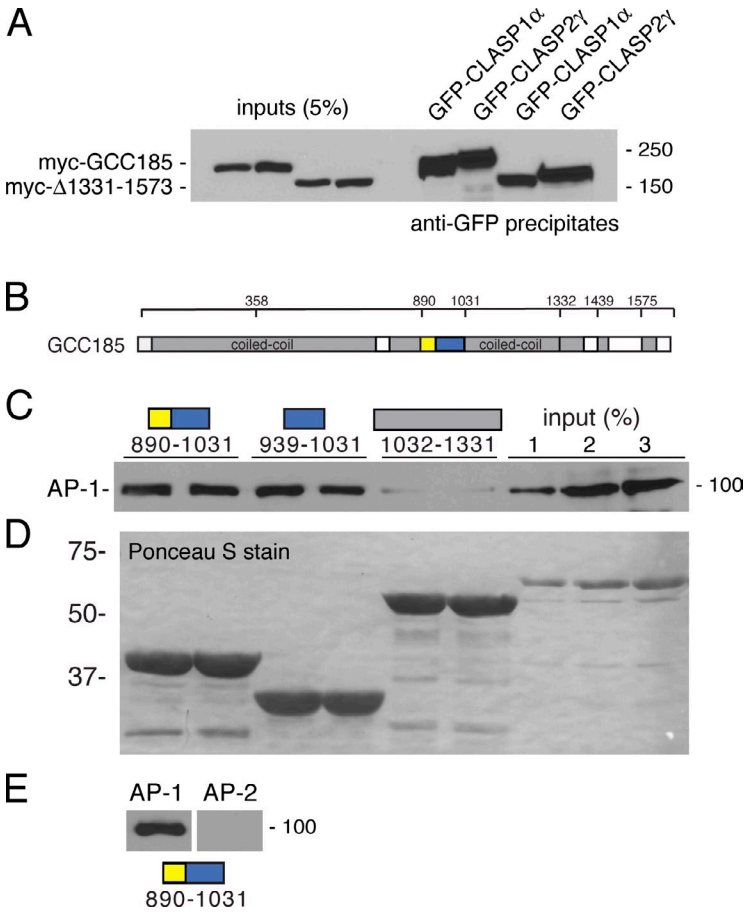

Figure 5. **The clathrin adaptor AP-1 binds the GCC185 coiled-coil domain required for vesicle tethering.** (A) CLASP coimmunoprecipitation with GCC185. HeLa cells expressing GFP–CLASP1-α or GFP–CLASP2-γ with either full-length myc-tagged GCC185 or myc-tagged GCC185 lacking residues 1,331–1,573 were lysed and incubated with NHS-Sepharose–coupled GFP-binding protein. Bound proteins were analyzed by SDS-PAGE and immunoblotting with anti-myc tag antibody. Left lanes, inputs (5%); right lanes, eluted samples. (B) A schematic diagram of GCC185 as shown in Fig. 3. (C) Binding of AP-1 to the indicated GCC185 constructs. Reactions contained 10 μM GST-GCC185 constructs and ~15 nM AP-1 purified from bovine brain membranes. Proteins were collected on glutathione-Sepharose, eluted with glutathione, and resolved by SDS-PAGE. Bound AP-1 was visualized by immunoblotting using 100/3 mouse anti–AP-1 γ-adaptin antibody (Sigma-Aldrich). (D) GCC185 constructs from reactions in B were visualized using Ponceau S staining. (E) 4 μM GST-tagged GCC185 890–1,031 was incubated with 390 nM of purified bovine AP-1 or 520 nM AP-2. Bound material was collected on glutathione-Sepharose beads, washed with 30 vol of binding buffer, and eluted with glutathione. Bound AP-2 was detected using 100/2 anti–α-adaptin antibody (Sigma-Aldrich). (C and E) In blue are residues 939–1,031; in yellow are residues 890–938, which represent a second region that is predicted to be unstructured. Molecular mass marker mobility is shown in kilodaltons.

Purified bovine brain AP-1 bound specifically to the construct containing residues 890–1,031 (Fig. 5 C, first and second lanes). Satisfyingly, full binding was also seen with the smaller GCC185 construct comprised of residues 939–1,031, which represents the precise domain needed for vesicle docking (Fig. 5 C, third and fourth lanes). Only background binding was detected when the adjacent coiled-coil residues 1,032–1,331 were tested (Fig. 5 C, fifth and sixth lanes). In addition, binding was specific for AP-1, as no binding was detected using purified AP-2 complexes (Fig. 5 E). These data show that the region of GCC185 needed for vesicle tethering (Fig. 5 B, blue box) can specifically bind AP-1 protein.

AP-1 is an exciting binding partner for several reasons. First, most tethers described to date bind to transport reaction–relevant coat proteins (Cai et al., 2007). Second, depletion of AP-1 leads to the accumulation of MPRs in early endosomes, supporting a role for this protein complex in MPR retrograde transport (Meyer et al., 2000). This latter result has been somewhat perplexing for many years, as AP-1 is localized primarily on the Golgi and is thought to catalyze MPR exit from the Golgi. If GCC185 binds AP-1 on inbound vesicles, these vesicles should be AP-1 decorated. This was tested directly in cells depleted of GCC185 under conditions in which MPRs accumulate in peripheral vesicles (Fig. 2 A; Reddy et al., 2006).

Fig. 6 shows deconvolution immunofluorescence microscopy images of peripheral transport intermediates that accumulate in GCC185-depleted (Fig. 6, B and D) but not control cells (Fig. 6, A and C). We have previously shown that a large proportion of these vesicles are Rab9 positive and that they lack the early endosome marker early endosome antigen 1 (EEA1; Reddy et al., 2006). Indeed, in triple-labeled deconvolution immunofluorescence microscopy experiments, 94% of 138 double-labeled MPR- and AP-1–positive vesicles lacked the EEA1 protein, supporting the conclusion that these are not early endosomes.

Because transport intermediates should be diffraction-limited spots by light microscopy, we first imaged 100-nm fluorescent beads and processed the images with a deconvolution algorithm to determine the range of pixel sizes that would roughly represent transport vesicles and not, for example, peripheral endosomes. 70% of the beads were detected within a range of 6–16 pixels in size; thus, this range was chosen to score vesicle-sized structures while excluding larger endosomes. Control HeLa cells showed very few peripheral vesicles containing MPRs, and only a small percentage of these objects also carried AP-1 (Fig. 6, A, C, and E). In GCC185-depleted cells, however, many peripheral MPR-containing vesicles were seen, and >30% of these vesicles also carried AP-1 (Fig. 6, B, D, and E).

Golgi-localized AP-1 and GCC185 represent distinct TGN domains

The finding that a block in transport vesicle tethering leads to the accumulation of MPRs in AP-1–coated transport intermediates strongly supports a role for AP-1 in retrograde transport.

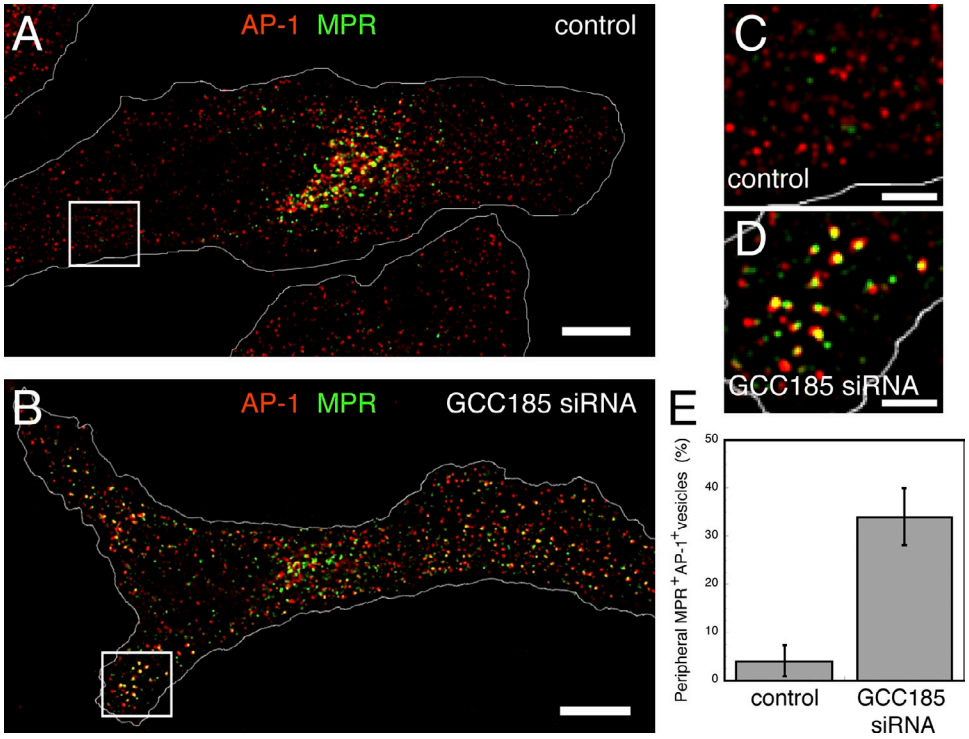

Figure 6. **AP-1 decorates transport vesicles that accumulate in cells depleted of GCC185.** (A and B) Deconvolved micrographs of cells either mock transfected (A) or transfected with GCC185 siRNA (B) labeled for MPR and AP-1. MPR localization was visualized using 2G11 mouse anti-MPR and Alexa Fluor 647 goat anti-IgG2$_a$ mouse antibodies. AP-1 was visualized using 100/3 mouse anti–AP-1 and Alexa Fluor 555 goat anti-IgG2$_b$ mouse antibodies. Approximate cell outlines are indicated. Bars, 10 µm. (C and D) Enlargement of the boxed regions in control (A) or GCC185-depleted (B) cells. Bars, 2.5 µm. (E) Quantification of the percentage of peripheral MPR-containing vesicles that also contain AP-1. For GCC185-depleted cells, 490 MPR$^+$ vesicles were counted from five cells from two independent experiments. For control cells, 76 MPR$^+$ peripheral vesicles were counted from four cells from three independent experiments. Error bars represent SEM.

But because AP-1 has long been associated with the formation of clathrin-coated vesicles at the TGN, we wanted to be sure that GCC185's capacity to bind AP-1 did not reflect an interaction of the two proteins within a common domain of the TGN that might be used during transport vesicle formation. Thus, we performed deconvolution microscopy to explore the localization of endogenous GCC185 and AP-1 proteins on the Golgi of BSc1 cells. As shown in Fig. 7, AP-1 was detected in small punctate structures, whereas GCC185 was entirely distinct and occupied a different highly reticular TGN microdomain. Similarly, the related GRIP domain containing the Golgin protein Golgin 245 was also reticular and was found adjacent to but not overlapping with GCC185, confirming the previously reported distinct localizations of these latter proteins (Derby et al., 2004). These data indicate that retrograde transport vesicles carrying MPRs dock at a domain that is spatially distinct from that used for MPR-containing transport vesicle formation. In addition, the data support the contention that AP-1 participates in retrograde transport of MPRs to the Golgi.

Discussion

We have shown, for the first time, that GCC185 contains two distinct functional domains that are needed to either maintain Golgi structure or to mediate transport vesicle consumption. Residues 939–1,031 are needed for tethering of MPR-containing vesicles to the Golgi but not for maintenance of Golgi structure, whereas residues 1,331–1,438 are needed for Golgi structure maintenance. This demonstrates that the two functions of the protein are separable. The region of GCC185 needed for vesicle tethering has the capacity to bind the clathrin adaptor AP-1 but not AP-2. This is exciting because most tethers bind to coat proteins corresponding to the transport step they catalyze; little was known previously about the coat that decorates MPR-containing vesicles inbound to the Golgi, and our finding led us to test whether these vesicles are, in fact, AP-1 coated. Indeed, in cells depleted of GCC185, MPRs accumulate in small vesicles that costain at a high frequency with anti–AP-1 antibodies.

AP-1 is highly enriched at the TGN as a result of strong binding interactions with phosphatidylinositol-4-phosphate (Wang et al., 2003) and Arf1 GTPase (Zhu et al., 1998). Immuno-EM has shown that MPR-containing clathrin-coated vesicles near the TGN are decorated with both AP-1 and so-called GGA proteins (Doray et al., 2002). Live-cell video microscopy has also detected AP-1 and GGA proteins on clathrin-coated structures that emanate from the TGN and deliver MPRs to early endosomes (Huang et al., 2001; Puertollano et al., 2003; Waguri et al., 2003; Polishchuk et al., 2006). These results support the conclusion that AP-1 functions in MPR export from the TGN to endosomes (Braulke and Bonifacino, 2009). Recent studies in *Drosophila* cells are entirely consistent with this conclusion and indicate that AP-1 and GGA proteins play redundant roles in MPR export (Hirst et al., 2009; Kametaka et al., 2010).

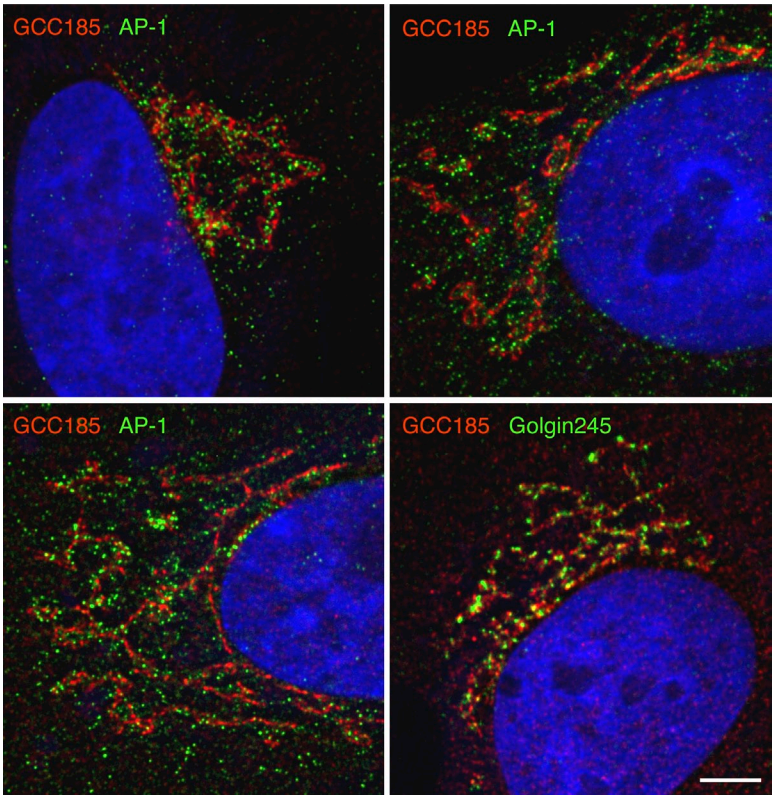

Figure 7. **AP-1 and GCC185 occupy distinct TGN microdomains.** Endogenous AP-1 or Golgin 245 and GCC185 were localized by deconvolution immunofluorescence microscopy. Bar, 5 µm.

Given AP-1's role in TGN export, it was at first surprising that AP-1 gene disruption led to the accumulation of MPRs in early endosomes (Meyer et al., 2000). This finding can be explained if GGAs, with or without AP-1, mediate TGN export of MPRs, whereas AP-1 (and not GGAs) functions in MPR transport both at the TGN and at endosomes. The conclusion that AP-1 plays a unique role at endosomes is supported by the observation that AP-1 depletion, but not GGA depletion, inhibits Nef-mediated downregulation of myosin heavy chain–class I (Hirst et al., 2009).

AP-1–mediated retrograde transport of MPRs from late endosomes to the TGN would be expected to involve a clathrin coat. Function-blocking X19 anticlathrin heavy chain antibodies failed to inhibit in vitro transport of MPRs from late endosomes to the TGN under conditions in which transferrin endocytosis was inhibited (Draper et al., 1990). Liu et al. (2001) have identified a novel clathrin isoform (CHC22) that is important for retrograde transport of proteins from endosomes to the Golgi (Esk et al., 2010). Depletion of CHC22 results in the redistribution of MPRs away from the perinuclear region (Esk et al., 2010). Unlike conventional clathrin (CHC17), CHC22 does not bind to light chains and is able to interact with AP-1 and AP-3 but not AP-2 complexes (Liu et al., 2001). X19 antibody fails to recognize CHC22 (Brodsky, F., personal communication), which would explain why X19 failed to inhibit MPR transport to the Golgi (Draper et al., 1990). Thus, CHC22, shown by Esk et al. (2010) to be important for MPR retrograde transport, likely functions in concert with AP-1 on the transport vesicles that we detected in cells depleted of GCC185 protein. AP-1 has the capacity to bind MPRs present in late endosomes and may work in concert with TIP47 and Rab9 proteins (Díaz and Pfeffer, 1998; Carroll et al., 2001) to package MPR cargo for export from late endosomes.

GCC185 is predicted to form a long structure that may extend 240 nm from the TGN surface (Hayes et al., 2009). Yet, the binding site that we have found necessary for vesicle docking (939–1,031) is located right in the middle of the protein. The presence of a nonessential Rab9 binding site immediately adjacent to the AP-1 binding site suggests that Rab9 binding may facilitate tethering by providing another vesicle-associated partner for GCC185 to bind to, even if that site is not required. The identification of these binding sites has provided an important clue to the nature of the vesicles that may be tethered; however, it does not provide an answer as to how the GCC185 protein accomplishes vesicle tethering. One possibility is that there is an additional transport vesicle binding site located closer to the N terminus. Given the presence of numerous Rab GTPase binding sites (Hayes et al., 2009) as well as binding sites for the target SNARE Syntaxin 16 (Ganley et al., 2008), it would not be surprising if additional binding sites are detected elsewhere in the protein. Importantly, the N-terminal 359 residues are essential for GCC185 function (Hayes et al., 2009), and the precise role of this domain deserves further analysis.

Our study shows that GCC185 does not need to be especially long to support Golgi ribbon structure maintenance. Although the protein is normally a dimer of 185-kD subunits, a smaller dimer comprised of two 130-kD chains was functional in this regard. GCC185 C-terminal determinants localize the protein on the Golgi and may also bind CLASP proteins that catalyze microtubule polymerization from the Golgi surface (Efimov et al., 2007). Residues 1,331–1,573 needed for normal Golgi ribbon morphology do not mediate CLASP binding; thus, another interaction must mediate this process.

Finally, deconvolution light microscopy has shown that GCC185 and Golgin 245 occupy distinct domains of the TGN, as originally detected by Derby et al. (2004). Importantly, TGN-associated AP-1 protein is distinct from domains decorated with either GCC185 or Golgin 245 protein (the latter shown indirectly). This indicates that transport vesicle–forming microdomains are adjacent to, but distinct from, regions that function in transport vesicle tethering. It will be of interest to determine whether these membrane domains are continuous or whether a fusion event is needed to bring recycled MPRs into vesicle-forming regions of the TGN. The localization of TGN clathrin in distal, nascent coated buds that are distinct from cisternal membranes has been seen in three-dimensional electron microscopic tomograms of the TGN (Fig. 9 in Ladinsky et al., 1999).

The process of transport vesicle tethering remains the least understood aspect of membrane traffic in eukaryotic cells. To serve as a tether, a protein must have the capacity to localize to a target membrane and reach out to interact with inbound transport vesicles. We have shown that GCC185 uses its C terminus to anchor at the Golgi via Rab6 and Arl1 GTPase binding. Here, we have identified a precise domain that can bind AP-1 on incoming transport vesicles and in some way facilitate the subsequent docking and fusion of these vesicles with their target. Future work will focus on conformational transitions taken by GCC185 to bring vesicle-associated SNARE proteins close enough to the target membrane to engage target SNAREs and permit membrane fusion.

Materials and methods

Expression plasmids

cDNAs encoding rescue plasmids were prepared with eight silent mutations in the siRNA-targeted region and ligated into pcDNA3.1(+) (Invitrogen) modified with an N-terminal myc tag as previously described (Hayes et al., 2009). The Δ359–XXX rescue constructs were prepared by concatenation of a PCR product encoding residues 34–358 with a GGATCC linker (AS) to sequences encoding the C terminus. These included Δ359–889 (34–358-AS-890–1,684), Δ359–1,030 (34–358-AS-1,031–1,684), Δ359–1,331 (34–358-AS-1,332–1,684), Δ359–1,438 (34–358-AS-1,439–1,684), and Δ359–1,574 (34–358-AS-1,575–1,674). The Δ1,331–1,573 rescue construct encoded residues 1–1,330 linked to 1,574–1,684. Δ889–1,032 encoded 1–888-LE-1,033–1,685. Δ889–939 encoded 1–888-LE-940–1,684. Δ938–1,032 encoded 1–937-LE-1,033–1,684. The Δ862–882 rescue construct encoded residues 1–861 concatenated to 883–1,684. Bacterial expression plasmids were prepared by ligating PCR products encoding residues 890–1,031, 890–1,331, 939–1,031, and 1,032–1,331 into the GST fusion vector pGEX4T-1 (GE Healthcare).

Cell culture, immunoblots, and immunoprecipitations

Cells were cultured at 37°C and 5% CO_2 in DME supplemented with 7.5% FBS, penicillin, and streptomycin. HEK293T cells were transfected with plasmids using polyethylenimine (Polysciences, Inc.). HeLa cells were transfected with GCC185 siRNA targeting the sequence 5′-GGAGTTGGAACAATCACAT-3′ using Oligofectamine (Invitrogen) according to the manufacturer's instructions. Mock treatment without siRNA was used as a negative control. siRNA-mediated depletion was performed for 72 h followed by fixation and staining. For rescue experiments, plasmids containing myc-tagged GCC185 constructs resistant to the siRNA were transfected using FuGENE6 (Roche) according to the manufacturer's instructions. For Fig. 1, rescue plasmids were transfected 48 h after initial siRNA treatment. For Figs. 2–4, rescue plasmids were transfected 24 h after initial siRNA treatment.

For immunoblots, cells expressing myc-GCC185 constructs for 48 h were washed twice in PBS and then lysed at 4°C in radioimmunoprecipitation assay buffer (Dintzis et al., 1994) containing protease inhibitors for 10 min. Lysates were clarified by centrifugation for 15 min at a relative centrifugal force of 16,000 at 4°C. Equal amounts of total lysate protein were analyzed by immunoblotting with the ECL Plus Western blotting detection system (GE Healthcare). For immunoprecipitations, HEK293T cells grown in 10-cm plates were transfected with the indicated GFP-CLASP and myc-GCC185 constructs. 36 h after transfection, cells were placed on ice, washed in PBS, and lysed in immunoprecipitation buffer (50 mM Hepes, pH 7.4, 150 mM KCl, 5 mM $MgCl_2$, 1 mM EDTA, and 1% Triton X-100) containing protease inhibitors at 4°C. Samples were centrifuged for 10 min at a relative centrifugal force of 16,000 at 4°C followed by preclearing with quenched *N*-hydroxysuccinimide (NHS)–Sepharose equilibrated in immunoprecipitation buffer for 30 min at 4°C. Samples were then incubated with 30 µl of 3-mg/ml NHS-immobilized GFP-binding protein (Rothbauer et al., 2008) for 1 h at 4°C. Bound material was washed four times in immunoprecipitation buffer and analyzed by SDS-PAGE and immunoblotting.

Protein expression, protein purification, and binding assays

GST-GCC185 constructs were transformed into BL21 (DE3) Rosetta II cells, and cultures (OD_{600} = 0.5) were induced with 0.2 mM IPTG for 2 h at 30°C. Cells were resuspended in 20 mM Tris, pH 7.4, 250 mM NaCl, 1 mM DTT, and 1 mM PMSF and lysed by two passes at >10,000 lb/in^2 in an EmulsiFlex-C5 apparatus (Avestin). Lysates were clarified by centrifugation twice at 20,000 rpm for 20 min each in a JA 20 rotor (Beckman Coulter). Clarified lysates were incubated with glutathione 4B–Sepharose beads (GE Healthcare) for 2 h at 4°C, washed with 100 vol of 20 mM Tris, pH 7.4, and 250 mM NaCl, and eluted with 20 mM Tris, pH 7.4, 250 mM NaCl, and 20 mM glutathione. Purified proteins were dialyzed against 20 mM Tris, pH 7.4, and 250 mM NaCl and then stored on ice to prevent freezing-induced aggregation.

AP-1 and AP-2 were purified according to Pauloin (1998) without the Mono Q step. Clathrin-coated vesicles were isolated by centrifugation through a sucrose cushion in D_2O. Coat proteins were released by incubation in 1 M Tris-HCl, pH 7.4, and adaptor proteins were resolved from clathrin using S-300 gel filtration. AP-1 was separated from AP-2 by hydroxyapatite chromatography. For binding assays (Fig. 5, C and D), ∼15 nM AP-1 was incubated with 10 µM GST-GCC185 domains in 20 mM Tris-HCl, pH 7.4, 250 mM NaCl, and 0.1% BSA for 60 min at 22°C. Bound product was collected on glutathione-Sepharose and washed with 120 column vol of 20 mM Tris-HCl, pH 7.4, 250 mM NaCl, and 1% CHAPS. Bound material was eluted with 20 mM Tris-HCl, pH 7.4, 250 mM NaCl, and 20 mM glutathione.

Immunofluorescence microscopy

Cell fixation, staining, and mounting in Mowiol were performed as previously described (Hayes et al., 2009). In brief, 24 h before fixation, cells were split onto 22 × 22–mm coverslips in a 6-well plate. Cells were washed twice in PBS and fixed for 20 min in 3.7% formaldehyde in 200 mM Hepes, pH 7.4. After fixation, cells were washed twice and incubated for 15 min in DME and 10 mM Hepes, pH 7.4, to quench. Cells were permeabilized for 5 min with 0.2% Triton X-100 in PBS followed by two washes and a 15-min incubation with 1% BSA in PBS. Monoclonal mouse anti–cation-independent MPR antibody (2G11; Lombardi et al., 1993), mouse anti–AP-1 (100/3, 1:1,000; Sigma-Aldrich), mouse anti–AP-2 (100/2, 1:1,000; Sigma-Aldrich), mouse anti-GM130 (1:500; BD), mouse anti–Golgin 245 (1:400; BD), mouse anti-EEA1 (1:1,000), rabbit anti-GCC185 (Reddy et al., 2006), and chicken anti-myc (1:750; Bethyl Laboratories, Inc.) primary antibodies were used. Alexa Fluor 488 goat anti–mouse (1:1,000), Alexa Fluor 568 goat anti–rabbit (1:1,000), Alexa Fluor 555 goat anti–chicken (1:2,000), Alexa Fluor 555 goat anti–mouse $IgG2_b$ (1:2,000), and Alexa Fluor 647 goat anti–mouse $IgG2_a$ (1:1,000) secondary antibodies were obtained from Invitrogen. Micrographs for Figs. 1–4 and 6 were acquired using a microscope (Eclipse 80i; Nikon) fitted with a 60×/NA 1.4 plan apochromat objective lens, a Sedat Quad filter set (Chroma Technology Corp.), and a charge-coupled device camera (CoolSnapHQ; Photometrics) at RT. Wavelength selection was performed using a controller (Lambda 10–3; Sutter Instrument). Z sections were acquired with a Z axis drive (MFC-2000; Applied Scientific Instrumentation) at 0.2-µm steps. All microscope instrumentation was controlled by MetaMorph imaging software (Molecular Devices). Micrographs for Fig. 7 were acquired at RT using a microscope (IX70; Olympus) fitted with a 100×/NA 1.4 plan apochromat objective lens, a Sedat Quad filter set (Semrock), and a charge-coupled device camera (CoolSnap HQ). All instrumentation was controlled by the integrated DeltaVision system (Applied Precision). Wavelength selection and z stack acquisition were performed using this system. Z sections were acquired at 0.2-µm steps. Images were deconvolved using a theoretical point spread function with softWoRx (v.4.1.0;

Applied Precision). For deconvolution micrographs in Fig. 6, the images displayed represent single slices of the z stack acquired. In Fig. 7, the deconvolution micrographs displayed represent projections of three to five central slices of the z stack acquired. For Golgi fragmentation and MPR dispersal phenotypes, cells were scored visually. To identify structures colabeled with AP-1 and MPR, objects between 6 and 16 pixels in size with >4 pixels of clear overlap were scored.

This research was supported by grants (GM079322 and DK37332) from the National Institutes of Health. F.C. Brown was supported in part by a National Institutes of Health training grant (T90DK070090).

Submitted: 6 April 2011
Accepted: 1 August 2011

References

Aivazian, D., R.L. Serrano, and S.R. Pfeffer. 2006. TIP47 is a key effector for Rab9 localization. *J. Cell Biol.* 173:917–926. doi:10.1083/jcb.200510010

Braulke, T., and J.S. Bonifacino. 2009. Sorting of lysosomal proteins. *Biochim. Biophys. Acta*. 1793:605–614. doi:10.1016/j.bbamcr.2008.10.016

Burguete, A.S., T.D. Fenn, A.T. Brunger, and S.R. Pfeffer. 2008. Rab and Arl GTPase family members cooperate in the localization of the golgin GCC185. *Cell*. 132:286–298. doi:10.1016/j.cell.2007.11.048

Cai, H., K. Reinisch, and S. Ferro-Novick. 2007. Coats, tethers, Rabs, and SNAREs work together to mediate the intracellular destination of a transport vesicle. *Dev. Cell*. 12:671–682. doi:10.1016/j.devcel.2007.04.005

Carroll, K.S., J. Hanna, I. Simon, J. Krise, P. Barbero, and S.R. Pfeffer. 2001. Role of Rab9 GTPase in facilitating receptor recruitment by TIP47. *Science*. 292:1373–1376. doi:10.1126/science.1056791

Derby, M.C., C. van Vliet, D. Brown, M.R. Luke, L. Lu, W. Hong, J.L. Stow, and P.A. Gleeson. 2004. Mammalian GRIP domain proteins differ in their membrane binding properties and are recruited to distinct domains of the TGN. *J. Cell Sci.* 117:5865–5874. doi:10.1242/jcs.01497

Derby, M.C., Z.Z. Lieu, D. Brown, J.L. Stow, B. Goud, and P.A. Gleeson. 2007. The trans-Golgi network golgin, GCC185, is required for endosome-to-Golgi transport and maintenance of Golgi structure. *Traffic*. 8:758–773. doi:10.1111/j.1600-0854.2007.00563.x

Díaz, E., and S.R. Pfeffer. 1998. TIP47: a cargo selection device for mannose 6-phosphate receptor trafficking. *Cell*. 93:433–443. doi:10.1016/S0092-8674(00)81171-X

Dintzis, S.M., V.E. Velculescu, and S.R. Pfeffer. 1994. Receptor extracellular domains may contain trafficking information. Studies of the 300-kDa mannose 6-phosphate receptor. *J. Biol. Chem.* 269:12159–12166.

Doray, B., P. Ghosh, J. Griffith, H.J. Geuze, and S. Kornfeld. 2002. Cooperation of GGAs and AP-1 in packaging MPRs at the trans-Golgi network. *Science*. 297:1700–1703. doi:10.1126/science.1075327

Draper, R.K., Y. Goda, F.M. Brodsky, and S.R. Pfeffer. 1990. Antibodies to clathrin inhibit endocytosis but not recycling to the trans Golgi network in vitro. *Science*. 248:1539–1541. doi:10.1126/science.2163108

Edeling, M.A., C. Smith, and D. Owen. 2006. Life of a clathrin coat: insights from clathrin and AP structures. *Nat. Rev. Mol. Cell Biol.* 7:32–44. doi:10.1038/nrm1786

Efimov, A., A. Kharitonov, N. Efimova, J. Loncarek, P.M. Miller, N. Andreyeva, P. Gleeson, N. Galjart, A.R. Maia, I.X. McLeod, et al. 2007. Asymmetric CLASP-dependent nucleation of noncentrosomal microtubules at the trans-Golgi network. *Dev. Cell*. 12:917–930. doi:10.1016/j.devcel.2007.04.002

Esk, C., C.Y. Chen, L. Johannes, and F.M. Brodsky. 2010. The clathrin heavy chain isoform CHC22 functions in a novel endosomal sorting step. *J. Cell Biol.* 188:131–144. doi:10.1083/jcb.200908057

Espinosa, E.J., M. Calero, K. Sridevi, and S.R. Pfeffer. 2009. RhoBTB3: a Rho GTPase-family ATPase required for endosome to Golgi transport. *Cell*. 137:938–948. doi:10.1016/j.cell.2009.03.043

Ganley, I.G., E. Espinosa, and S.R. Pfeffer. 2008. A syntaxin 10-SNARE complex distinguishes two distinct transport routes from endosomes to the trans-Golgi in human cells. *J. Cell Biol.* 180:159–172. doi:10.1083/jcb.200707136

Ghosh, P., N.M. Dahms, and S. Kornfeld. 2003. Mannose 6-phosphate receptors: new twists in the tale. *Nat. Rev. Mol. Cell Biol.* 4:202–212. doi:10.1038/nrm1050

Glickman, J.N., E. Conibear, and B.M. Pearse. 1989. Specificity of binding of clathrin adaptors to signals on the mannose-6-phosphate/insulin-like growth factor II receptor. *EMBO J.* 8:1041–1047.

Hayes, G.L., F.C. Brown, A.K. Haas, R.M. Nottingham, F.A. Barr, and S.R. Pfeffer. 2009. Multiple Rab GTPase binding sites in GCC185 suggest a model for vesicle tethering at the trans-Golgi. *Mol. Biol. Cell*. 20:209–217. doi:10.1091/mbc.E08-07-0740

Hirst, J., D.A. Sahlender, M. Choma, R. Sinka, M.E. Harbour, M. Parkinson, and M.S. Robinson. 2009. Spatial and functional relationship of GGAs and AP-1 in *Drosophila* and HeLa cells. *Traffic*. 10:1696–1710. doi:10.1111/j.1600-0854.2009.00983.x

Huang, F., A. Nesterov, R.E. Carter, and A. Sorkin. 2001. Trafficking of yellow-fluorescent-protein-tagged mu1 subunit of clathrin adaptor AP-1 complex in living cells. *Traffic*. 2:345–357. doi:10.1034/j.1600-0854.2001.25020506.x

Kametaka, S., N. Sawada, J.S. Bonifacino, and S. Waguri. 2010. Functional characterization of protein-sorting machineries at the trans-Golgi network in *Drosophila melanogaster*. *J. Cell Sci.* 123:460–471. doi:10.1242/jcs.055103

Ladinsky, M.S., D.N. Mastronarde, J.R. McIntosh, K.E. Howell, and L.A. Staehelin. 1999. Golgi structure in three dimensions: functional insights from the normal rat kidney cell. *J. Cell Biol.* 144:1135–1149. doi:10.1083/jcb.144.6.1135

Liu, S.H., M.C. Towler, E. Chen, C.Y. Chen, W. Song, G. Apodaca, and F.M. Brodsky. 2001. A novel clathrin homolog that co-distributes with cytoskeletal components functions in the trans-Golgi network. *EMBO J.* 20:272–284. doi:10.1093/emboj/20.1.272

Lombardi, D., T. Soldati, M.A. Riederer, Y. Goda, M. Zerial, and S.R. Pfeffer. 1993. Rab9 functions in transport between late endosomes and the trans Golgi network. *EMBO J.* 12:677–682.

Luke, M.R., L. Kjer-Nielsen, D.L. Brown, J.L. Stow, and P.A. Gleeson. 2003. GRIP domain-mediated targeting of two new coiled-coil proteins, GCC88 and GCC185, to subcompartments of the trans-Golgi network. *J. Biol. Chem.* 278:4216–4226. doi:10.1074/jbc.M210387200

Meyer, C., D. Zizioli, S. Lausmann, E.L. Eskelinen, J. Hamann, P. Saftig, K. von Figura, and P. Schu. 2000. mu1A-adaptin-deficient mice: lethality, loss of AP-1 binding and rerouting of mannose 6-phosphate receptors. *EMBO J.* 19:2193–2203. doi:10.1093/emboj/19.10.2193

Miller, P.M., A.W. Folkmann, A.R. Maia, N. Efimova, A. Efimov, and I. Kaverina. 2009. Golgi-derived CLASP-dependent microtubules control Golgi organization and polarized trafficking in motile cells. *Nat. Cell Biol.* 11:1069–1080. doi:10.1038/ncb1920

Pauloin, A. 1998. Clathrin-coated vesicles and targeting. Preparation of adaptor proteins. *Methods Mol. Biol.* 88:275–284.

Pfeffer, S.R. 2010. How the Golgi works: a cisternal progenitor model. *Proc. Natl. Acad. Sci. USA*. 107:19614–19618. doi:10.1073/pnas.1011016107

Polishchuk, R.S., E. San Pietro, A. Di Pentima, S. Teté, and J.S. Bonifacino. 2006. Ultrastructure of long-range transport carriers moving from the trans Golgi network to peripheral endosomes. *Traffic*. 7:1092–1103. doi:10.1111/j.1600-0854.2006.00453.x

Puertollano, R., N.N. van der Wel, L.E. Greene, E. Eisenberg, P.J. Peters, and J.S. Bonifacino. 2003. Morphology and dynamics of clathrin/GGA1-coated carriers budding from the trans-Golgi network. *Mol. Biol. Cell*. 14:1545–1557. doi:10.1091/mbc.02-07-0109

Reddy, J.V., A.S. Burguete, K. Sridevi, I.G. Ganley, R.M. Nottingham, and S.R. Pfeffer. 2006. A functional role for the GCC185 golgin in mannose 6-phosphate receptor recycling. *Mol. Biol. Cell*. 17:4353–4363. doi:10.1091/mbc.E06-02-0153

Riederer, M.A., T. Soldati, A.D. Shapiro, J. Lin, and S.R. Pfeffer. 1994. Lysosome biogenesis requires Rab9 function and receptor recycling from endosomes to the trans-Golgi network. *J. Cell Biol.* 125:573–582. doi:10.1083/jcb.125.3.573

Rothbauer, U., K. Zolghadr, S. Muyldermans, A. Schepers, M.C. Cardoso, and H. Leonhardt. 2008. A versatile nanotrap for biochemical and functional studies with fluorescent fusion proteins. *Mol. Cell. Proteomics*. 7:282–289.

Sinka, R., A.K. Gillingham, V. Kondylis, and S. Munro. 2008. Golgi coiled-coil proteins contain multiple binding sites for Rab family G proteins. *J. Cell Biol.* 183:607–615. doi:10.1083/jcb.200808018

Waguri, S., F. Dewitte, R. Le Borgne, Y. Rouillé, Y. Uchiyama, J.F. Dubremetz, and B. Hoflack. 2003. Visualization of TGN to endosome trafficking through fluorescently labeled MPR and AP-1 in living cells. *Mol. Biol. Cell*. 14:142–155. doi:10.1091/mbc.E02-06-0338

Wang, Y.J., J. Wang, H.Q. Sun, M. Martinez, Y.X. Sun, E. Macia, T. Kirchhausen, J.P. Albanesi, M.G. Roth, and H.L. Yin. 2003. Phosphatidylinositol 4 phosphate regulates targeting of clathrin adaptor AP-1 complexes to the Golgi. *Cell*. 114:299–310. doi:10.1016/S0092-8674(03)00603-2

Zhu, Y., L.M. Traub, and S. Kornfeld. 1998. ADP-ribosylation factor 1 transiently activates high-affinity adaptor protein complex AP-1 binding sites on Golgi membranes. *Mol. Biol. Cell*. 9:1323–1337.